ACS APPLIED MATERIALS & INTERFACES

Research Article

www.acsami.org

Encapsulating Gold Nanoparticles or Nanorods in Graphene Oxide Shells as a Novel Gene Vector

Cheng Xu,[†,‡] Darong Yang,[‡] Lin Mei,[†,‡] Bingan Lu,[†,‡] Libao Chen,[†,‡] Qiuhong Li,*[,†,‡] Haizhen Zhu,*[,‡] and Taihong Wang*[,†,‡]

[†]Key Laboratory for Micro-Nano Optoelectronic Devices of Ministry of Education and [‡]State Key Laboratory for Chemo/Biosensing and Chemometrics, Hunan University, Changsha, 410082, P. R. China

Supporting Information

ABSTRACT: Surface modification of inorganic nanoparticles (NPs) is extremely necessary for biomedical applications. However, the processes of conjugating ligands to NPs surface are complicated with low yield. In this study, a hydrophilic shell with excellent biocompatibility was successfully constructed on individual gold NPs or gold nanorods (NRs) by encapsulating NPs or NRs in graphene oxide (GO) nanosheets through electrostatic self-assembly. This versatile and facile approach remarkably decreased the cytotoxicity of gold NPs or NRs capping with surfactant cetyltrimethylammonium bromide (CTAB) and provided abundant functional groups on NPs surface for further linkage of polyethylenimine (PEI). The PEI-functionalized GO-encapsulating gold NPs (GOPEI-AuNPs) were applied to delivery DNA into HeLa cells as a novel gene vector. It exhibited high transfection efficiency of 65% while retaining 90% viability of HeLa cells. The efficiency was comparable to commercialized PEI 25 kDa with the cytotoxicity much less than PEI. Moreover, the results on transfection efficiency was higher than PEI-functionalized GO, which can be attributed to the small size of NPs/DNA complex (150 nm at the optimal w/w ratio) and the spherical structure facilitating the cellular uptake. Our work paves the way for future studies focusing on GO-encapsulating, NP-based nanovectors.

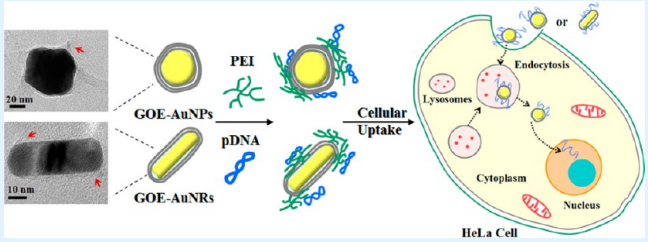

KEYWORDS: *graphene oxide, gold nanoparticles, gold nanorods, gene delivery, core/shell materials*

1. INTRODUCTION

As the success of gene therapy is highly dependent on the delivery carrier, research in this field have been focused on the development of a safe and efficient delivery system.[1] Inorganic nanoparticles (NPs) including gold,[2−5] silica,[6−8] and iron oxide[9,10] are promising nonviral gene delivery vectors because of their unique optical, magnetic and chemical properties. However, many of them are insoluble and easy to aggregate in biological media, which severely limits their biomedical applications. So a wide range of ligation and encapsulation methods have been developed to render NPs soluble in aqueous solution, prevent aggregation and provide anchor points where functional molecules can be attached.[11−13] Among these methods, encapsulation of NPs by an inorganic,[14] lipidic,[15,16] or mesoporous carbon[17] shell has significant advantages over directly conjugating surface ligands on NPs, because the encapsulating shells are more stable and even strong thiol ligands can dissociate from or undergo exchange on gold surfaces.[13] In addition, the processes of conjugating ligands are usually complicated, and low-yielding.[18]

Graphene oxide (GO), a novel carbon nanomaterial prepared from natural graphite, has attracted great attention in biomedical applications such as drug[19−21] and gene[22−24] delivery, protein delivery,[25,26] and imaging in vitro.[27] Recent studies demonstrated that polymer-functionalized GO such as polyethylenimine (PEI)-[22−24] or chitosan-functionalized[28] GO can be well-dispersed in physiological solution and efficiently delivery DNA or siRNA into cancer cells.[29,30] Zhou et al.[31] reported that the gene delivery system based on ultrasmall GO could be more efficient than commercial Lipofectamine and PEI (60 kDa) both in mammalian cell lines and zebrafish embryos. For the practical application of GO, the biosafety aspect of GO was investigated by some groups.[32,33] Ruiz et al.[34] demonstrated that GO almost had no intrinsic cytotoxic properties in mammalian cells and acted as a general enhancer of cellular growth. Zhang et al.[35] reported that GO obviously cleared from the mouse body within a week and no pathological changes were observed.

On the other hand, GO possesses unique features such as facile synthesis, high dispersibility in water, prominent flexibility, easily tunable surface functionalization and good biocompatibility, which make it highly suitable to be the shell materials for encapsulating NPs. Gold nanoparticles (AuNPs) have long been regarded as alternate nonviral vectors for transporting and loading genes.[36] AuNPs conjugates can be delivered systemically, eliciting low immunogenic responses and demonstrating long circulatory half-lives.[37,38] In addition, they possesses several advantages as cores such as bioinertia

Received: January 17, 2013
Accepted: March 11, 2013
Published: March 11, 2013

and nontoxicity.[39] More importantly, the AuNPs' size and shape as well as the surface charge are controllable,[40,41] making them facile for further encapsulation. The cetyltrimethylammonium bromide (CTAB) has been widely used as a surfactant in the synthesis of AuNPs and gold nanorods (AuNRs). Nevertheless, CTAB remained on the surface of AuNPs and AuNRs are toxic to cells,[42] and hard to be removed completely. The encapsulation by GO will not only decrease the toxicity of AuNPs and AuNRs with residual CTAB but also provide functional groups on the surface for further modification.

The fabrication of graphene-encapsulating AuNPs was reported by some groups with a chemical vapor deposition (CVD) process.[43,44] However, it involved high growth temperatures with low yield, and it is inconvenient to collect the products from the substrate, limiting its biomedical applications. Recently some investigators developed more facile and green approaches for encapsulating NPs by GO through electrostatic self-assembly in solution.[45,46] Yang et al.[47] demonstrated that GO and metal oxides can coassemble into core/shell hybrids under electrostatic forces. Myung et al.[48] fabricated a reduced GO-encapsulating SiO_2 NPs based biosensor. The surface of SiO_2 NPs was modified by positively charged molecules and then encapsulated by negatively charged GO sheets. This encapsulation approach was economic with low energy consumption. But the products reported by these groups involved the encapsulation of multinanoparticles or large nanoparticles (>200 nm) with poor dispersibility, and it is difficult for them to enter into cells. As far as we know, there is no related report about GO-encapsulating NPs as nanovectors for gene delivery.

Herein, we describe a general strategy for the fabrication of GO-encapsulating gold nanoparticles (GOE-AuNPs) or gold nanorods (GOE-AuNRs) by electrostatic self-assembly between negatively charged GO nanosheets[49] and positively charged gold nanoparticles. In the resulting GOE-AuNPs and GOE-AuNRs, ultrathin GO shells effectively enwrapped every individual nanoparticle with excellent dispersibility. Next, we graft the cationic polymer polyethylenimine (PEI) onto the GO surface using an amide linkage, making it available for gene delivery. This unique structure can (1) suppress the aggregation of GO sheets or gold nanoparticles; (2) provide anchor points for further functional modification; (3) condense the plasmid DNA onto the surface of NPs. As a consequence, it was found that the PEI-functionalized GO-encapsulating AuNPs (GOPEI-AuNPs) presented much lower cytotoxicity and comparable transfection efficiency with commercial PEI 25 kDa and higher efficiency than PEI-fuctionalized GO[24] in HeLa cells.

2. MATERIALS AND METHODS

2.1. Materials. Native graphite flake was purchased from Alfa Aesar. Branched polyethylenimine (25000 Da) and N-(3-dimethylaminopropyl)-N′-ethylcarbodiimide hydrochloride (EDC) were purchased form Sigma-Aldrich. $HAuCl_4$, $AgNO_3$ and $NaBH_4$ were purchased from Sinopharm Chemical Reagent Co. Ltd., China. [3-(4,5-dimethylthiazol-2-yl)-5-(3-carboxymethoxyphenyl)-2-(4-sulfophenyl)-2H-tetrazolium, inner salt; MTS] and plasmid DNA pGL-3 were obtained from Promega and directly used. CTAB and RPMI-1640 medium were purchased from Dingguo Biotech. Co. Ltd., Beijing. Plasmid DNA (pSuper.retro.neo+gfp) was purchased from Oligoengine Co. Ltd. Other chemicals mentioned in this article were purchased from Sinopharm Chemical Reagent Co. Ltd., China, with analytical grade and used as received. Milli-Q water was used in all experiments.

2.2. Preparation of GOE-AuNPs and GOE-AuNRs. GO was prepared by Hummers method,[49] then exfoliated into GO nanosheets (see the Supporting Information). The gold nanoparticles[41] and nanorods[38] were synthesized by using the same surfactant CTAB (SI). The GOE-AuNPs and GOE-AuNRs were fabricated via an electrostatic interaction. In a typical process, 5 mL AuNPs or AuNRs aqueous dispersion (1.4 mg/mL) were added into a 30 mL aqueous GO suspension (0.05 mg/mL) and mildly magneticly stirred for 1h. The GOE-AuNPs or GOE-AuNRs were obtained by centrifugation (8000 rpm for 10 min) and redispersed in deionized water.

2.3. Preparation of GOPEI-AuNPs and GOPEI-AuNRs. Branched PEI 25 kDa was grafted to GOPEI-AuNPs by an amide bond between PEI and GOPEI-AuNPs in the presence of EDC and NHS. In a typical procedure, an aqueous solution of PEI (25 mg, dissolved in 5 mL distilled water) and EDC (0.025 g) were added to GOE-AuNPs solution (0.5 mg/mL, 20 mL). After stirred for 30 min, additional EDC (0.07 g) and NHS (0.11 g) were added and stirred overnight. After the reaction was terminated, the mixture was filtered via a 100 K ultrafilter. The retainer in the ultrafilter was repeatedly washed with aqueous solution containing 10% NaCl and 10% urea to remove any unreacted PEI. Free PEI in the ultrafiltrate was detected by ninhydrin to confirm complete removal of unreacted PEI. Finally, the collected solid was redispersed and dialyzed (MWCO = 8 kDa) against distilled water for 3 days at 4 °C to remove NaCl and urea, and it formed a stable solution (about 1.6 mg/mL GOPEI-AuNPs). The approach described above was applied to the preparation of GOPEI-AuNRs and GOPEI.

2.4. Characterization. The samples were characterized by scanning electron microscope (SEM, Hitachi S-4800) and transition electron microscope (TEM, JEM-2100F, 200 kV). The UV−vis absorption spectra were recorded by a spectrometer UV1601 (SHIMADZU Co. Ltd.). The samples for FT-IR were prepared in KBr pellets. Thermogravimetric analysis (TGA) data were achieved on a Netzsch STA449C in O_2 atmosphere at a heating rate of 10 °C/min from 30 to 900 °C. DLS (dynamic light scattering) and zeta potential analysis were performed using a Malvern Zetasizer Nano 3000 HS (Malvern, Worcestershire, England). The concentration of PEI 25 kDa in the GOPEI-AuNPs or GOPEI-AuNRs complex were estimated by measuring the cuprammonium complex formed between PEI and copper ion(II) at 630 nm using UV−vis spectrophotometry.[23] Core/shell complex to DNA ratios are expressed as weight ratios of GOPEI-AuNPs or GOPEI-AuNRs to DNA (w/w ratios). GOPEI-AuNPs/pDNA or GOPEI-AuNRs/pDNA complex at various w/w ratios were prepared by adding appropriate volumes of GOPEI-AuNPs or GOPEI-AuNRs solution to 1 mg of pDNA solution, followed by vortexing for 60 s and incubating at room temperature for 30 min. The solution was then diluted to 2 mL for size and zeta potential measurements, and all data were averaged over three measurements.

2.5. Cell Culture and Cytotoxicity Assay. Human cervical carcinoma cells HeLa were maintained in a RPMI-1640 medium supplemented with 10% fetal bovine serum (FBS). Cells were seeded in tissue culture flasks (about 3×10^5 cells) and incubated in a fully humidified atmosphere at 37 °C with 5% CO_2. For the MTS assay, HeLa cells were separately seeded into 96-well plates at a density of 5000 cells/well and cultured for 24 h in 100 μL of complete RPMI-1640. The GOPEI-AuNPs or GOPEI-AuNRs solution were added in each well and incubated for another 24 h. The medium was replaced by 100 μL fresh RPMI-1640. Then, 20 μL MTS solution was added and incubated for 1 h. The absorbance was measured at 490 nm using a microplate reader (Thermo Multiskan MK3). The relative cell viability was calculated according to the following equation:

$$\text{relative cell viability (\%)} = 100 \times (OD_{test} - OD_0)/(OD_{control} - OD_0)$$

OD_{test} was the optical density of the cell solution cultured with GOPEI-AuNPs or GOPEI-AuNRs. $OD_{control}$ was the optical density of the cell solution in the absence of GOPEI-AuNPs and GOPEI-AuNRs. OD_0 was the optical density of the solution containing cells without MTS. The morphology images of HeLa cells after separately incubated

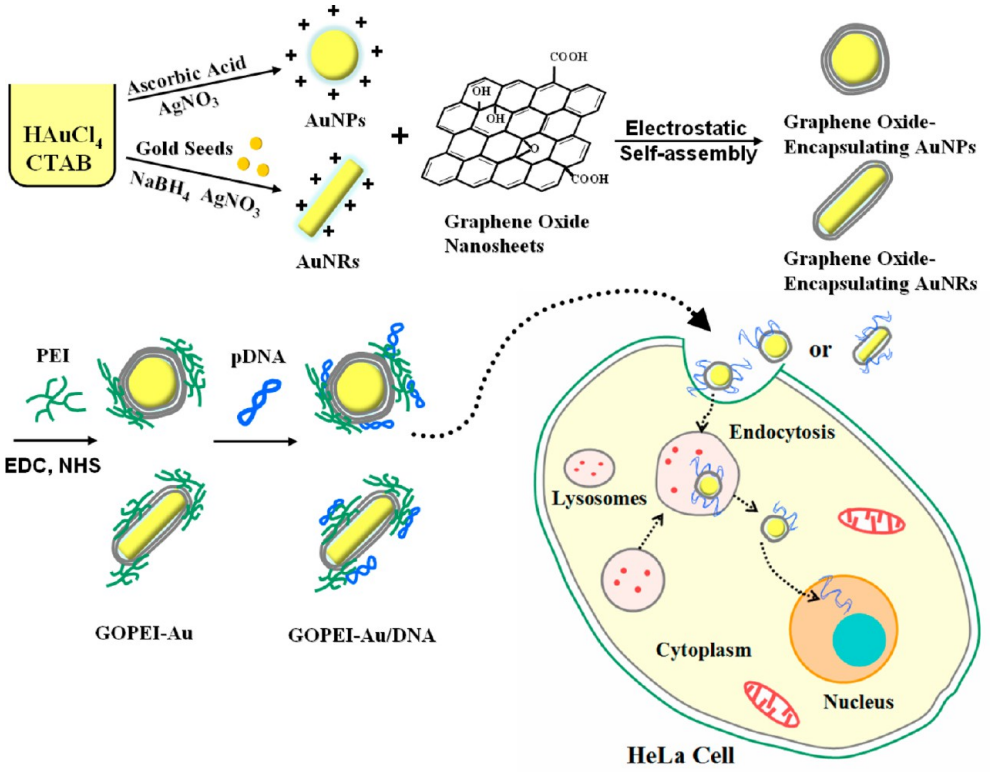

Figure 1. Schematic illustration for the synthesis of GOPEI-AuNPs and GOPEI-AuNRs, and the possible mechanism of gene delivery in HeLa cells by using GOPEI-AuNPs as carrier.

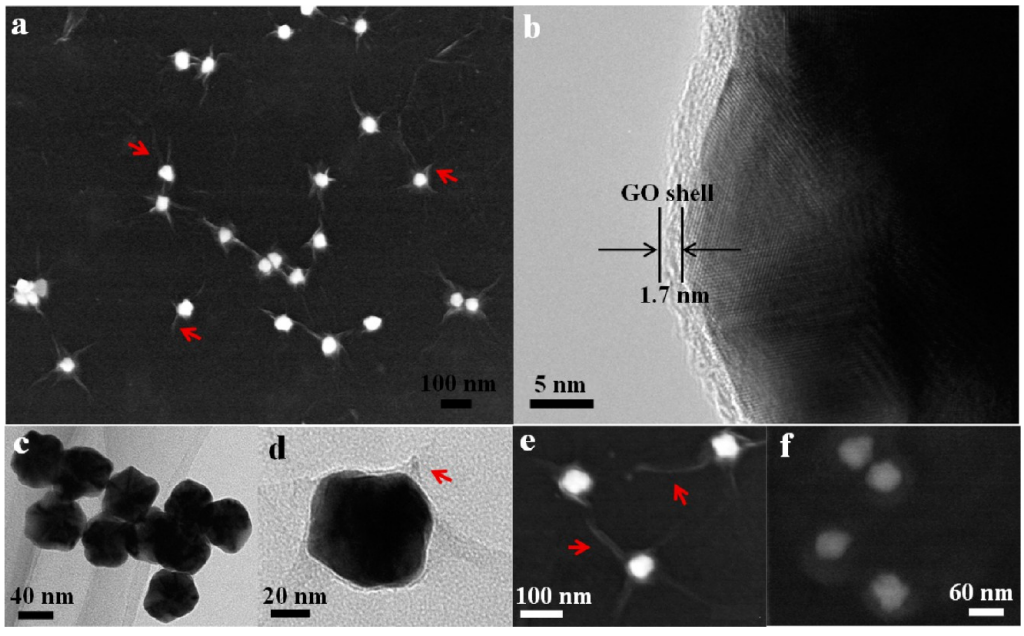

Figure 2. Morphology and structure of the AuNPs, GOE−AuNPs and GOPEI-AuNPs. (a, e) SEM images, (b) HRTEM image, and (d) TEM image of the as-obtained GOE-AuNPs. (c) TEM image of AuNPs and (f) SEM image of GOPEI-AuNPs. The redundant GO shells could be observed from the edges of the particles. The red arrows pointed to the presence of the redundant GO shells.

with 10 mg/L AuNPs, AuNRs, GOE-AuNPs and GOE-AuNRs for 24 h were undertaken on an Olympus IX71 fluorescence microscope. To remove excess CTAB, AuNPs and AuNRs were washed for 3 times with deionized water by centrifugation (8000 rpm for 10 min).

2.6. In vitro Gene Transfection Assay. GOPEI-AuNPs/pDNA or GOPEI-AuNRs/pDNA complex were formed by adding appropriate volumes of GOPEI-AuNPs or GOPEI-AuNRs solution to 1 mg of pDNA solution, followed by vortexing for 60 s and incubating at room temperature for 30 min. All of the complexes were prepared and used immediately.

GOPEI-AuNPs/pDNA complexes for agarose gel electrophoresis were prepared with different weight ratios of 0:1, 0.05:1, 0.15:1, 0.3:1, 0.75:1, and 1.5:1. In general, different amounts of GOPEI-AuNPs solution were mixed with 1 μg of pDNA solution, followed by incubated for half hour at room temperature. Ten μL of the complex was electrophoresed in 0.9% (w/v) agarose with a TAE buffer at 120 V

dx.doi.org/10.1021/am400212j | ACS Appl. Mater. Interfaces 2013, 5, 2715−2724

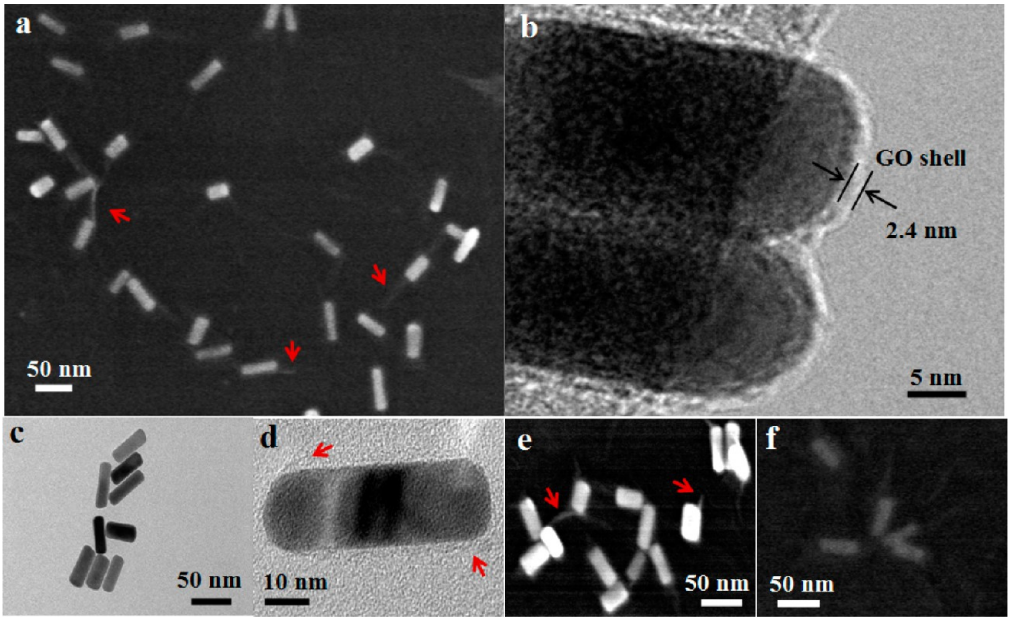

Figure 3. Morphology and structure of the AuNRs and GOE−AuNRs. (a, e) SEM images, (b, d) TEM image of the as-obtained GOE-AuNRs. (c) TEM image of AuNRs and (f) SEM image of GOPEI-AuNRs. The red arrows pointed to the presence of the redundant GO shell "tails".

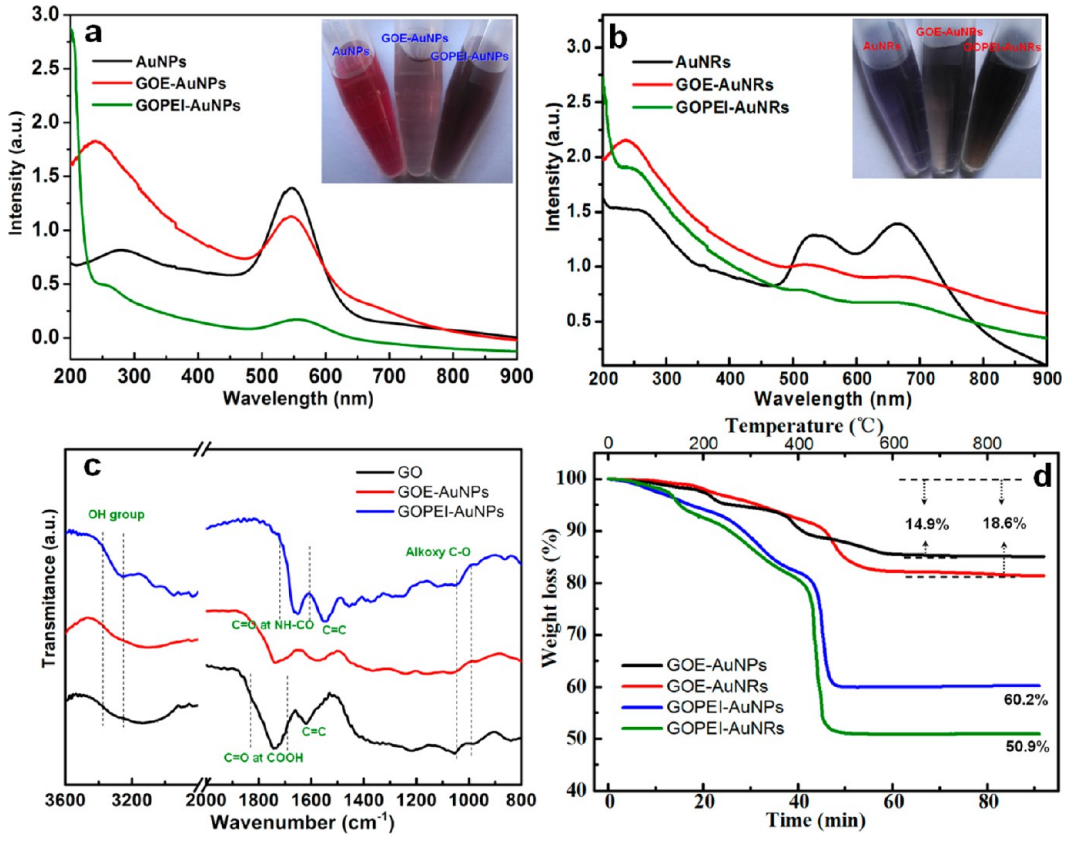

Figure 4. (a) UV−vis absorption spectra and a photograph (inset) of the AuNPs, GOE-AuNPs and GOPEI-AuNPs. (b) UV−vis absorption spectra and a photograph (inset) of the AuNRs, GOE-AuNRs and GOPEI-AuNRs. (c) FT-IR spectroscopy of the GO, GOE-AuNPs and GOPEI-AuNPs. (d) Thermogravimetric analysis curve of the GOE-AuNPs, GOE-AuNRs, GOPEI-AuNPs, and GOPEI-AuNRs at a heating rate of 10 °C per min in oxygen.

for 30 min with the electrophoresis apparatus (Tanon EPS300). DNA bands were visualized by a gel image system, Tanon 2500R.

For in vitro transfection studies with expressing green fluorescent protein (GFP), cells were seeded into 24-well plates at a density of 5×10^4 cells/well in 1 mL of RPMI-1640 containing antibiotics for 24 h prior to transfection. At the time of transfection, the medium in each well was replaced by 0.5 mL of RPMI-1640 without FBS. Twenty μL complex containing 1 μg of plasmid DNA were added to each well and incubated with the cells for 4 h under a standard culture condition. Then the medium was replaced by 0.5 mL of fresh complete RPMI-

1640 and cells were further incubated for 20 h under the same condition, resulting in a total transfection time of 24 h. The cells expressing GFP were observed by an Olympus IX71 fluorescence microscope.

For the quantitative transfection efficiency experiments, Luciferase gene pGL-3 was used as reporter gene. The HeLa cells were seeded on 24-well plates at an initial density of 5×10^4 cells/well and incubated for 24 h in 1 mL of RPMI-1640 containing 10% FBS at 37 °C in a humidified atmosphere with 5% CO_2 before transfection. At the time of transfection, the medium in each well was replaced by 0.5 mL of RPMI-1640 medium without FBS. The 20 μL pDNA complex with 1 μg of pDNA at different weight ratios were then added into the wells, and incubated in 500 μL of serum-free medium for 4 h under a standard culture condition. Then the medium was replaced by 1 mL of fresh complete RPMI-1640 and cells were further incubated for 44 h under the same condition, resulting in a total transfection time of 48 h. The luciferase assay was carried out according to the supplier's protocol (Promega), and relative luciferase activity was measured on a single-well luminometer (LB9507, Berthold Co. Ltd.) for 10 s.

3. RESULTS AND DISCUSSION

3.1. Synthesis and Characterization of GOE-AuNPs and GOPEI-AuNPs. As shown in Figure 1, the major emphasis of this study was 4-fold: (1) synthesis of positively charged AuNPs or AuNRs in controllable sizes and shapes by using the same surfactant CTAB; (2) fabrication of GO-encapsulating AuNPs or AuNRs by mutual electrostatic interactions; (3) the cationic polymer PEI was then connected to the surface of GOE-AuNPs and GOE-AuNRs via an amide linkage between amino groups on PEI and carboxylic groups on GO, to afford GOPEI-AuNPs or GOPEI-AuNRs; (4) the GOPEI-AuNPs and GOPEI-AuNRs were then loaded with plasmid DNA (pDNA) by electrostatic interaction. In our strategy, we used GOPEI-AuNPs/pDNA or GOPEI-AuNRs/pDNA to transfect the human cervical carcinoma cell line HeLa, and examined the transfection efficiency and toxicity by green fluorescent protein (GFP) expression assay, luciferase report gene assay, and MTS assay.

Table 1. Characteristics of Synthesized Gold-GO Core/Shell Complex

	degree of GO[a] (mass fraction) (%)	degree of gold (mass fraction) (%)	degree of PEI[b] (mass fraction) (%)
GOE-AuNPs	14.9	85.1	0
GOE-AuNRs	18.6	81.4	0
GOPEI-AuNPs	11.1	60.2	28.7
GOPEI-AuNRs	13.7	50.9	35.4
GOPEI	21.7	0	78.3

[a]The concentration of GO in GOE-AuNPs or GOE-AuNRs was determined by thermogravimetric analysis under oxygen atmosphere. [b]The concentration of PEI 25 kDa in the GOPEI-AuNP or GOPEI-AuNR complex was estimated by measuring the cuprammonium complex formed between PEI and copper ion(II) at 630 nm using UV−vis spectrophotometry.[23] (See Figure S3 in the Supporting Information.)

The morphology and structure of the AuNPs, GOE−AuNPs, and GOPEI-AuNPs were elucidated by scan electron microscope (SEM), transmission electron microscope (TEM) and high-resolution TEM (HRTEM) measurements. It can be seen that the AuNPs were fairly uniform in size and shape with diameters of 50−60 nm (Figure 2c). The SEM and TEM images of the GOE-AuNPs clearly showed that they had a rough and crinkled surface, which was associated with the presence of flexible and ultrathin graphene sheets. In most cases, the redundant GO shells could be observed from the edges of the particles (Figure 2a, d, e). Remarkably, the GO effectively enwrapped every individual gold nanoparticle and isolated from each other. By using this method, AuNPs were largely (>85%) singly encapsulated in GO nanosheets. The thickness of GO shell was about 1.7 nm, as measured from HR-TEM (Figure 2b). The GO shells on the surface of NPs contributed to the enhancement of biocompatibility and provided functional groups for further modification. After conjugated PEI molecules, the NPs surface became blurred in SEM image (Figure 2f).

Such an assembly protocol can be further extended to the construction of other GO-encapsulating nanomaterials with different morphologies as long as they had similar positively charged surface. The AuNRs synthesized by surfactant CTAB were about 50 nm length and 15 nm in diameter (Figures 3c). The SEM and TEM images of the GOE-AuNRs (Figure 3a, b, d, e) and GOPEI-AuNRs (Figure 3f) showed that one or two gold nanorods were encapsulated in GO with redundant GO shell "tails". These "tails" definitely reflected the presence of flexible GO nanosheets. It demonstrated that NPs with different shapes can be successfully encapsulated by GO nanosheets in our approach.

The GOE-AuNPs and GOE-AuNRs were studied by the UV−vis absorption spectra, as shown in panels a and b in Figure 4. The UV−vis absorption peak at 545 nm, originating from the AuNPs coating with the surfactant CTAB, remained essentially unchanged.[44] The absorption peak for both GOE-AuNPs and GOPEI-AuNPs was at 239 nm, which was the characteristic absorption peak of GO. The existence of GO led to a solution color change that was visible to eyes (Figure 4a, inset). The functional groups on GO surface and covalent attachment of PEI onto GO via amide linkage were confirmed by Fourier transform infrared (FT-IR) spectroscopy, as shown in Figure 4c. The FT-IR spectroscopy revealed the existence of OH (3400 cm^{-1}), C═O (1733 cm^{-1}), and C═C (1580 cm^{-1}) functional groups in GO and GOE-AuNPs, which indicated that identical oxygen functional groups and sp^3 defects existed in both GO and GOE-AuNPs. The appearance of vibration band around 1650 cm^{-1} due to the C═O stretching of primary amide in GOPEI-AuNPs and the disappearance of carboxylic group bands at 1733 cm^{-1} of pristine GO substantiated the formation of amide linkages.

The sizes and surface charge of AuNPs, GOE-AuNPs, and GOPEI-AuNPs were investigated by the dynamic light scattering (DLS) and zeta potential measurements. As shown in Figure S1a (Supporting Information), the average size of original AuNPs was about 62.6 nm. The average hydrodynamic radius of GO nanosheets was about 113.8 nm (see Figure S2b in the Supporting Information). After encapsulated by GO nanosheets, the average size of AuNPs increased to 89.4 nm. When grafted PEI onto the GO surface, the size of GOPEI-AuNPs was increased to 130.7 nm. The change in surface charge of AuNPs was shown in Figure S1a inset. The initial surface charge of the AuNPs was positively charged (zeta potential = 6.6 mV), attributing to the residual surfactant CTAB on the AuNPs surface. After encapsulated by GO, the surface charge of GOE-AuNPs was negatively charged (zeta potential = −30.1 mV). Apparently, this charge originated from

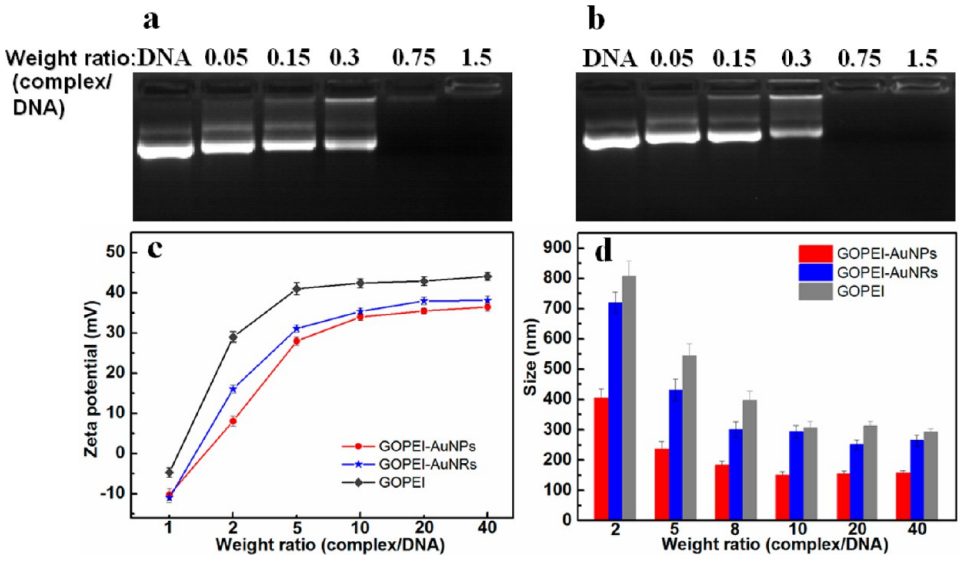

Figure 5. Agarose gel electrophoresis assay of (a) GOPEI-AuNPs/pDNA complex and (b) GOPEI-AuNRs/pDNA complex at various weight ratios. (c) Zeta potential of GOPEI-AuNPs/DNA, GOPEI-AuNRs/DNA, and GOPEI/DNA complex at different weight ratios. (d) Variation in particle size of GOPEI-AuNPs/DNA, GOPEI-AuNRs/DNA and GOPEI/DNA complex at different weight ratios. Data represent mean values for $n = 3$ and bars are standard deviations for means.

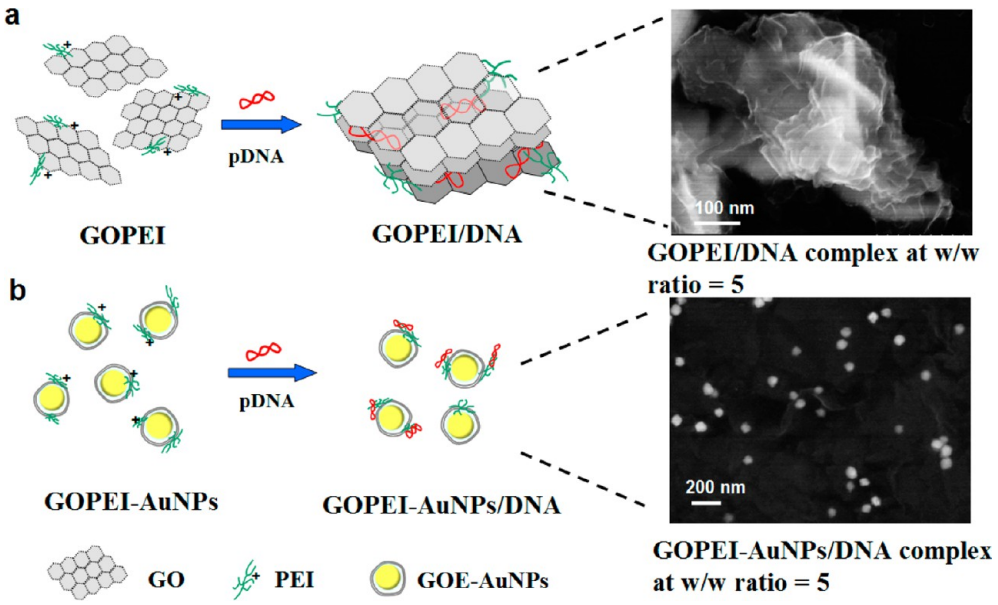

Figure 6. Possible mechanism of (a) GOPEI and (b) GOPEI-AuNPs interacting with pDNA at low weight ratios and the SEM images of (a) GOPEI/pDNA and (b) GOPEI-AuNPs/pDNA complex at the w/w ratio of 5:1.

the ionization of the carboxylic acid and phenolic hydroxy groups that were located on the GO. The surface charge switched from negative to positive (zeta potential = 36.9 mV) after conjugated PEI. The change in size and surface charge originated from layer-by-layer self-assembly of GO and PEI, which was observed in the same way as the encapsulation of AuNRs (see Figure S1b in the Supporting Information).

Thermogravimetric analysis (TGA) of GOE−AuNPs (Figure 4d) and GOE-AuNRs revealed that the weight fraction of GO was 14.9% and 18.8% respectively, which were higher than those of reported graphene-encapsulating-nanoparticles composites (4−9%).[47] The high content of GO would improve the biocompatibility and water solubility of the composite and provide more anchor points for grafting cationic PEI subsequently. The concentration of PEI 25 kDa in the GOPEI-AuNPs or GOPEI-AuNRs complex were 28.7 and 35.4%, respectively (Table 1). The relatively low concentration of PEI made the complex less toxicity to the cell.

3.2. GOPEI-AuNPs/pDNA and GOPEI/pDNA Complex. Recently, some groups have demonstrated that PEI-functionalized GO (GOPEI) exhibited an excellent ability to condense DNA into nanosized complex.[24] In this section, we compared our GOPEI-AuNPs and GOPEI-AuNRs with GOPEI in the DNA-condensation capacity by zeta potential measurements and DLS.

To study pDNA loading on GOPEI-AuNPs or GOPEI-AuNRs, an agarose gel electrophoresis assay was carried out after the incubation of GOPEI-AuNPs or GOPEI-AuNRs with pDNA at different weight ratios. Images a and b in Figure 5 showed that the migration of pDNA was retarded completely

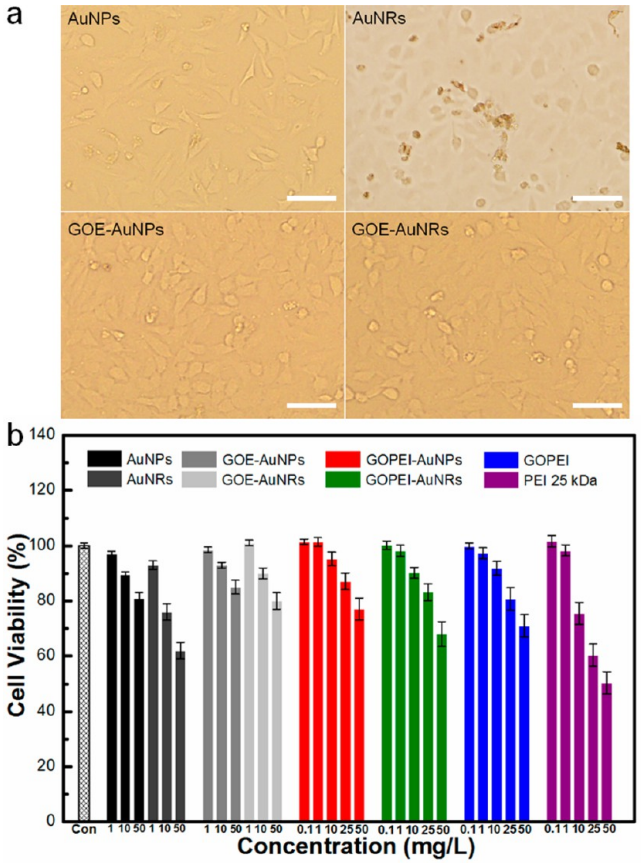

Figure 7. (a) Morphology of HeLa cells after incubated with 10 mg/L AuNPs (CTAB-capped), AuNRs (CTAB-capped), GOE-AuNPs and GOE-AuNRs respectively for 24h. The scale bars in the figure are 50 μm. (b) Cytotoxicity of AuNPs (CTAB-capped), AuNRs (CTAB-capped), GOE-AuNPs, GOE-AuNRs, GOPEI-AuNPs, GOPEI-AuNRs, GOPEI, and PEI to HeLa cells. The relative percentage of the control cells not exposed to the transfection system (nontreated) was used to represent 100% cell viability. To remove excess CTAB, we washed AuNPs and AuNRs 3 times with deionized water by centrifugation (8000 rpm for 10 min). Data represent mean values for n = 3 and bars are standard deviations for means.

when the weight ratio (w/w ratio) of GOPEI-AuNPs or GOPEI-AuNRs to pDNA was higher than 1.5: 1.

The surface charge of NPs/pDNA complex greatly affected DNA-condensation capacity and transfection efficiency. Therefore, the surface charges of GOPEI-AuNPs/pDNA, GOPEI-AuNRs/pDNA and GOPEI/pDNA complex at different weight ratios were investigated by zeta potential measurements. As shown in Figure 5c, the zeta potential of GOPEI-AuNPs/pDNA was negative at a low weight ratio of 1:1, indicating incomplete DNA condensation. With increasing weight ratios, the zeta potential rose dramatically and reached a plateau around 36.5 mV. The GOPEI/pDNA complex exhibited a higher positive zeta potential than GOPEI-AuNPs/pDNA at every w/w ratio because of the higher content of PEI molecules. The positively charged surface of NPs/pDNA complex facilitated their attachment to the negatively charged cellular membranes resulting in the promotion of cellular uptake.

To gain efficient endocytosis and gene transfer, the complex should be small and compact. The size distribution of GOPEI-AuNPs/pDNA, GOPEI-AuNRs/pDNA and GOPEI/pDNA complexes at various w/w ratios were characterized by DLS. As shown in Figure 5d, the average size of GOPEI-AuNPs/pDNA was 405.2 nm at a low w/w ratio of 2:1, indicating incomplete condensation of pDNA. The efficiency of pDNA condensation rose with increasing weight ratios and the size of the nanocomplex was 150.1 nm at the w/w ratio of 10:1. Remarkably, the average size of GOPEI-AuNPs/pDNA was much smaller than that of GOPEI/pDNA and GOPEI-AuNRs/pDNA complexes over the entire range of weight ratios. After incubation with pDNA at the w/w ratio of 5:1 for 1h, the average size for GOPEI/pDNA complex increased to 550 nm, implying the formation of aggregate. GOPEI-AuNPs/pDNA and GOPEI/pDNA complexes at the w/w ratio of 5:1 were investigated by SEM for further studies. The SEM image of GOPEI/pDNA aggregate (Figure 6a) showed a typical multilayer-stacked morphology. On the basis of the experimental evidence from DLS and SEM, the reason for aggregation was schematically illustrated (Figure 6a). Several pieces of GOPEI sheets aggregated together by the electrostatic force between negative charged pDNA and positively charged GOPEI sheets and formed a layered bionanostrucute[50] with average size of 500−600 nm, which was consistent with some previous reports.[23,24] The GOPEI/pDNA aggregate was difficult to enter the cells, which would decrease the transfection efficiency. Nevertheless, no obvious aggregation was observed from the SEM image of GOPEI-AuNPs/pDNA complex (Figure 6b), and they were well dispersed and isolated from each other. It was probably because the contact area between GOPEI-AuNPs spheres was much smaller than that between GOPEI sheets. As a result, compared with GOPEI sheets and GOPEI-AuNRs (see Figure S4 in the Supporting Information), the GOPEI-AuNPs of spherical structure was able to prevent aggregation and condensate pDNA into a smaller, more compact nanocomplex, facilitating cellular internalization.

3.3. Cell Toxicity and In Vitro Transfection. For the practical application in gene delivery, an acceptable safety profile was the most important.[51] In this study, cytotoxicity was evaluated by both morphological observation of cells with a bright field microscopy (Figure 7a) and MTS viability assays (Figure 7b). As shown in Figure 7a, cells incubated with the 10 mg/L AuNRs for 24 h separated from each other in a shrinking morphology and some dead cells were found in sight. However, no obvious morphological change of HeLa cells was observed in the presence of GOE-AuNPs or GOE-AuNRs, which highlighted the excellent biocompatibility of GO shells. The cytotoxicity of GOPEI-AuNPs and GOPEI-AuNRs to HeLa cells was assessed by the MTS assay by comparison with original AuNPs, AuNRs, GOE-AuNPs, GOE-AuNRs, GOPEI and branched PEI 25 kDa, as shown in Figure 7b. The results suggested that without surface modification or encapsulation by GO, the AuNPs and AuNRs with residual CTAB appeared to be rather toxic to Hela cells. Especially the AuNRs synthesized in a high concentration of CTAB, killed almost half of cells at a concentration of 50 mg/L. After encapsulated by GO, the toxicity to HeLa cells were significantly reduced, in good agreement with microscopic results. The PEI exhibited the highest cytotoxicity over the whole concentration range. GOPEI-AuNPs and GOPEI-AuNRs showed a significantly lower cytotoxicity than PEI, which was attributed to the decreased charge density of the composites by distributing PEI molecules on GO surface.[52] Even at a GOPEI-AuNPs concentration as high as 50 mg/L, the relative cell viability was still higher than 80%, while the viability of HeLa cells with

dx.doi.org/10.1021/am400212j | ACS Appl. Mater. Interfaces 2013, 5, 2715−2724

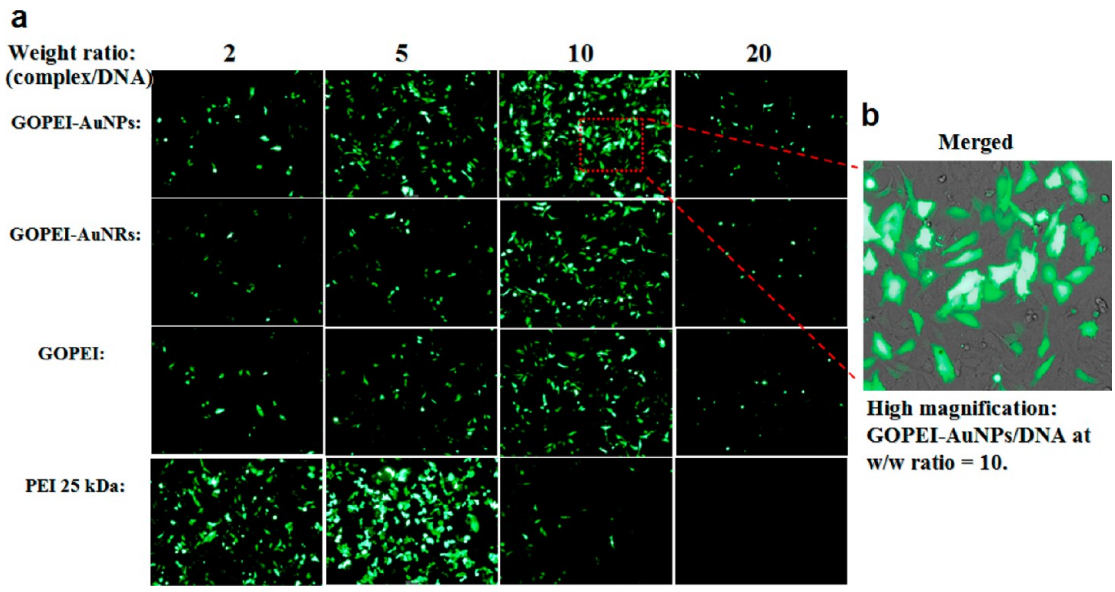

Figure 8. (a) Fluorescence microscopy images of HeLa cells transfected with GOPEI-AuNPs, GOPEI-AuNRs, GOPEI and branched PEI 25 kDa at different weight ratios in GFP expression experiment. The scale bars in the figures are 100 μm. (b) Merged fluorescence image showed transfected cells expressing GFP internalizing with GOPEI-AuNPs (w/w ratio =10) with a high magnification. The scale bar in the figure is 20 μm.

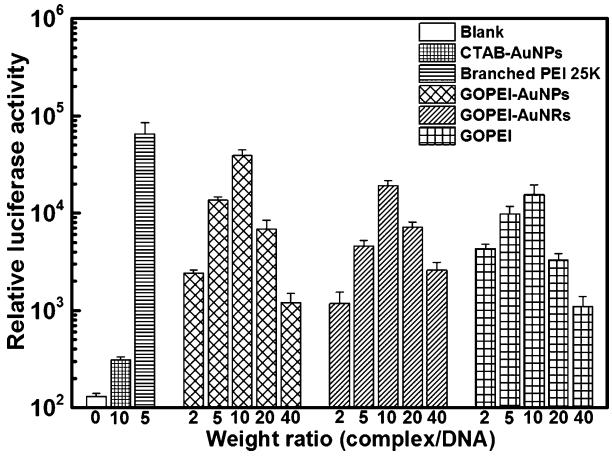

Figure 9. Tansfection experiment of GOPEI-AuNPs and GOPEI-AuNRs in HeLa cells at diffierent weight ratios with luciferase reporter gene. PEI 25 kDa at its optimal w/w ratio = 5 and original AuNPs (CTAB-capped) were used as controls. Luciferase reporter gene expression was evaluated by using a microplate spectrofluorometer. Data represent mean values for n = 3 and bars are standard deviations for means.

GOPEI and PEI was about 68 and 50%, respectively. This implied the great potential of GOPEI-AuNPs as a nonviral gene carrier with a high biosafety and low toxicity.

In vitro transfection with GOPEI-AuNPs/pDNA or GOPEI-AuNRs/pDNA complexes to HeLa cells was conducted to directly visualize the transfected cells expressing GFP at weight ratios from 2 to 20. For comparison, branched PEI 25 kDa and GOPEI were used as controls. The transfected cells with expressing GFP were observed by a reverse fluorescence microscope. The results in Figure 8a revealed that, at the optimal w/w ratio of 10:1, we observed a strikingly high transfection efficiency of GOPEI-AuNPs with about 65% cells expressing GFP, and the natural cellular morphology were observed (Figure 8b). The PEI showed high transfection efficiency at a low w/w ratio but almost no GFP expression at a high w/w ratio of 20, because of the low viability of the cells. The GFP expression of GOPEI-AuNPs was significantly higher than GOPEI at each w/w ratio, which indicated that GOPEI-AuNPs was a more efficient carrier for transporting DNA in HeLa cells. In addition, the transfection efficiency of GOPEI-AuNRs was lower than GOPEI-AuNPs from the GFP expression since the spherical morphology was more facile for cellular endocytosis according to previous reports.[53,54]

For the quantitative transfection efficiency experiments of GOPEI-AuNPs and GOPEI-AuNRs, luciferase was used as a reporter gene in HeLa cells. The primal CTAB-capped AuNPs (CTAB-AuNPs) and branched PEI 25 kDa at its optimal w/w = 5 were used as controls. Figure 9 showed that CTAB-AuNPs with pDNA almost had no transfection efficiency, probably because it could not load large amount of pDNA. The branched PEI 25 kDa possessed the highest transfection efficiency as before. Its relative luciferase activity reach up to 6.5 × 10^4, but significant cytotoxicity of PEI should be considered carefully in biomedical applications. The transfection efficiency mediated by GOPEI-AuNPs was still higher than GOPEI and GOPEI-AuNRs. At the optimal w/w ratio of 10, the relative luciferase activity of GOPEI-AuNPs was about 4 × 10^4, whereas the activity for GOPEI-AuNRs and GOPEI was 1.9× 10^4 and 1.5× 10^4, respectively. The high transfection efficiency of GOPEI-AuNPs was own to the smaller particle size and the spherical structure of GOPEI-AuNPs facilitating cellular uptake. Although the transfection efficiency was not superior to that of commercial vector PEI 25 kDa, our GOPEI-AuNPs and GOPEI-AuNRs possessed much less cytotoxicity which was extremely necessary for clinical use of nonviral gene vector. More importantly, these results evidently suggested the great promise of this versatile approach for constructing biocompatible and hydrophilic surface on NPs as an efficient gene vector.

4. CONCLUSIONS

In summary, we have constructed a highly biocompatible and hydrophilic shell on individual gold nanoparticle and nanorod surface by encapsulating NPs or NRs in GO nanosheets and

used these core/shell hybrids for the first time as gene vectors to delivery pDNA into HeLa cells. It exhibited good DNA-binding capacity and condensed plasmid DNA into nanoscale particles (150 nm). In vitro gene transfection tests demonstrated that GOPEI-AuNPs presented much lower cytotoxicity and comparable transfection efficiency (65% efficiency and 90% viability) with commercial PEI 25 kDa and higher efficiency than GOPEI in HeLa cells, which can be attributed to the small size and spherical structure facilitating cellular uptake. Considering the excellent dispersibility, biocompatibility and high transfection efficiency of GOPEI-AuNPs and GOPEI-AuNRs, their applications can be extended to siRNA delivery and photothermal therapy. Furthermore, by using this method, a variety of NPs with specific function can be encapsulated in a biocompatible and hydrophilic shell, which will promote the development of novel nanovectors based on GO-encapsulating NPs for biomedical applications.

■ ASSOCIATED CONTENT

Ⓢ Supporting Information

Description related to synthesis of GO nanosheets, AuNPs, AuNRs, DLS, and zeta measurements results of gold-GO core/shell complex (Figure S1), the characterization of GO nanosheets (Figure S2), the standard curve of PEI 25 kDa concentration (Figure S3), the SEM image of GOPEI-AuNRs/pDNA complex at the w/w ratio of 5:1 (Figure S4), and the cytotoxicity of GO nanosheets to Hela cells (Figure S5). This material is available free of charge via the Internet at http://pubs.acs.org/.

■ AUTHOR INFORMATION

Corresponding Author

*E-mail: liqiuhong2004@hotmail.com (Q.L.); zhuhaizhen69@yahoo.com (H.Z.); thwang@aphy.iphy.ac.cn (T.W.). Tel./ Fax: +86-0731- 88664019.

Notes

The authors declare no competing financial interest.

■ ACKNOWLEDGMENTS

We thank the financial support of the National Natural Science Foundation of China (Grant 21003041 and 21103046) and the Hunan Provincial Natural Science Foundation of China (Grant 10JJ1011 and 11JJ7004).

■ REFERENCES

(1) Li, S. D.; Huang, L. *Gene Ther.* **2006**, *13*, 1313.
(2) Arvizo, R. R.; Bhattacharyya, S.; Kudgus, R. A.; Giri, K.; Bhattacharya, R.; Mukherjee, P. *Chem. Sov. Rev.* **2012**, *41*, 2943.
(3) Yan, X. H.; Blacklock, J.; Li, J. B.; Mohwald, H. *ACS Nano* **2012**, *6*, 111.
(4) Thomas, M.; Klibanov, A. M. *Proc. Natl. Acad. Sci. U.S.A.* **2003**, *100*, 9138.
(5) Zhao, E. Y.; Zhao, Z. X.; Wang, J. C.; Yang, C. H.; Chen, C. J.; Gao, L. Y.; Feng, Q.; Hou, W. J.; Gao, M. Y.; Zhang, Q. *Nanoscale* **2012**, *4*, 5102.
(6) Hartono, S. B.; Gu, W.; Kleitz, F.; Liu, J.; He, L.; Middelberg, A. P. J.; Yu, C.; Lu, G. Q.; Qiao, S. Z. *ACS Nano* **2012**, *6*, 2104.
(7) Kim, M. H.; Na, H. K.; Kim, Y. K.; Ryoo, S. R.; Cho, H. S.; Lee, K. E.; Jeon, H.; Ryoo, R.; Min, D. H. *ACS Nano* **2011**, *5*, 3568.
(8) Shen, S.; Gu, T.; Xiao, X.; Yuan, P.; Yu, M.; Xia, L.; Ji, Q.; Meng, L.; Song, W.; Yu, C.; Lu, G. *Chem. Mater.* **2012**, *24*, 230.
(9) Kievit, F. M.; Veiseh, O.; Fang, C.; Bhattarai, N.; Lee, D.; Ellrnbogen, R. G.; Zhang, M. *ACS Nano* **2010**, *4*, 4587.
(10) Sun, S.; Lo, Y.; Chen, H.; Wang, L. *Langmuir* **2012**, *28*, 3542.
(11) Xu, Y.; Qin, Y.; Palchoudhury, S.; Bao, Y. *Langmuir* **2011**, *27*, 8990.
(12) Fang, C.; Bhattarai, N.; Sun, C.; Zhang, M. *Small* **2009**, *5*, 1637.
(13) Chen, H. Y.; Abraham, S.; Mendenhall, J.; Delmarre, S. C.; Smith, K.; Kim, I.; Batt, C. A. *ChemPhysChem* **2008**, *9*, 388.
(14) Su, Y. Y.; He, Y.; Lu, H. T.; Sai, L. M.; Li, Q. N.; Li, W. X.; Wang, L. H.; Shen, P. P.; Huang, Q.; Fan, C. H. *Biomaterials* **2009**, *30*, 19.
(15) Dubertret, B.; Skourides, P.; Norris, D. J.; Noireaux, V.; Brivanlou, A. H.; Libchaber, A. *Science* **2002**, *298*, 1759.
(16) Koole, R.; van Schooneveld, M. M.; Hihorst, J.; Castermans, K.; Cormode, D. P.; Strijkers, G. J.; Donega, C. M.; Vanmaekelbergh, D.; Griffioen, A. W.; Nicolay, K.; Fayad, Z. A.; Meijerink, A.; Mulder, W. J. M. *Bioconjugate Chem.* **2008**, *19*, 2471.
(17) Chopra, N.; Bachas, L. G.; Knecht, M. R. *Chem. Mater.* **2009**, *21*, 1176.
(18) Kievit, F. M.; Wang, F. Y.; Fang, C.; Mok, H.; Wang, K.; Silber, J. R.; Ellenbogen, R. G.; Zhang, M. Q. *J. Controlled Release* **2011**, *152*, 76.
(19) Zhang, L. M.; Xia, J. G.; Zhao, Q. H.; Liu, L. W.; Zhang, Z. J. *Small* **2010**, *6*, 537.
(20) Liu, Z.; Robinson, J. T.; Sun, X. M.; Dai, H. J. *J. Am. Chem. Soc.* **2008**, *130*, 10876.
(21) Pandey, H.; Parashar, V.; Parashar, R.; Prakash, R.; Ramtekea, P. W.; Pandeyb, A. C. *Nanoscale* **2011**, *3*, 4104.
(22) Feng, L. Z.; Zhang, S.; Liu, Z. *Nanoscale* **2011**, *3*, 1252.
(23) Kim, H.; Namgung, R.; Singha, K.; Oh, I. K.; Kim, W. J. *Bioconjugate Chem.* **2011**, *22*, 2558.
(24) Chen, B.; Liu, M.; Zhang, L. M.; Huang, J.; Yao, J. L.; Zhang, Z. J. *J. Mater. Chem.* **2011**, *21*, 7736.
(25) Shen, H.; Liu, M.; He, H. X.; Zhang, L. M.; Huang, J.; Chong, Y.; Dai, J. W.; Zhang, Z. J. *ACS Appl. Mater. Interfaces* **2012**, *4*, 6317.
(26) Mu, Q. X.; Su, G. X.; Li, L. W.; Gilbertson, B. O.; Yu, L. H.; Zhang, Q.; Sun, Y.; Yan, B. *ACS Appl. Mater. Interfaces* **2012**, *4*, 2259.
(27) Sun, X. M.; Liu, Z.; Welsher, K.; Robinson, J. T.; Goodwin, A.; Zaric, S.; Dai, H. J. *Nano Res.* **2008**, *1*, 203.
(28) Bao, H.; Pan, Y.; Ping, Y.; Sahoo, N. G.; Wu, T.; Li, L.; Li, J.; Gan, L. H. *Small* **2011**, *7*, 1569.
(29) Zhang, L. M.; Lu, Z. X.; Zhao, Q. H.; Huang, J.; Shen, H.; Zhang, Z. J. *Small* **2011**, *4*, 460.
(30) Yang, X. Y.; Niu, G. L.; Cao, X. F.; Wen, Y. K.; Xiang, R.; Duan, H. Q.; Chen, Y. S. *J. Mater. Chem.* **2012**, *22*, 6649.
(31) Zhou, X.; Laroche, F.; Lamers, G. E. M.; Torraca, V.; Voskamp, P.; Lu, T.; Chu, F. Q.; Spaink, H. P.; Abrahams, J. P.; Liu, Z. F. *Nano Res.* **2012**, *5*, 703.
(32) Liao, K. H.; Lin, Y. S.; Macosko, C. W.; Haynes, C. L. *ACS Appl. Mater. Interfaces* **2011**, *3*, 2607.
(33) Lu, B. A.; Li, T.; Zhao, H. T.; Li, X. D.; Gao, C. T.; Zhang, S. X.; Xie, E. Q. *Naoscale* **2012**, *4*, 2978.
(34) Ruiz, O. N.; Fernando, K. A. S.; Wang, B. J.; Brown, N. A.; Luo, P. G.; Mcnamara, N. D.; Vangsness, M.; Sun, Y. P.; Bunker, C. E. *ACS Nano* **2011**, *5*, 8100.
(35) Zhang, X. Y.; Yin, J. L.; Peng, C.; Hu, W. P.; Zhu, Z. Y.; Li, W. X.; Fan, C. H.; Huang, Q. *Carbon* **2011**, *49*, 986.
(36) Ghosh, P. S.; Kim, C. K.; Han, G.; Forbes, N. S.; Rotello, V. M. *ACS Nano* **2008**, *2*, 2213.
(37) Dreaden, E. C.; Mackey, M. A.; Huang, X.; Kang, B.; Ei-Sayed, M. A. *Chem. Soc. Rev.* **2011**, *40*, 3391.
(38) Xu, L. G.; Liu, Y.; Chen, Z. Y.; Li, W.; Liu, Y.; Wang, L. M.; Liu, Y.; Wu, X. C.; Ji, Y. L.; Zhao, Y. L.; Ma, L. Y.; Shao, Y. M.; Chen, C. Y. *Nano Lett.* **2012**, *12*, 2003.
(39) Han, L.; Zhao, J.; Zhang, X.; Cao, W. P.; Hu, X. X.; Zou, G. Z.; Duan, X. L.; Liang, X. J. *ACS Nano* **2012**, *6*, 7340.
(40) Sau, T. K.; Murphy, C. J. *J. Am. Chem. Soc.* **2004**, *126*, 8648.
(41) Zheng, P. C.; Hu, J.; Shen, G. L.; Jiang, J. H.; Yu, R. Q.; Liu, G. K. *Chin. J. Chem.* **2009**, *27*, 2137.
(42) Niidome, T.; Yamagata, M.; Okamoto, Y.; Akiyama, Y.; Takahashi, H.; Kawano, T.; Katayama, Y.; Niidome, Y. *J. Controlled Release* **2006**, *114*, 343.

(43) Wu, J. C.; Chopra, N. *Processing of Nanoparticle Materials and Nanostructured Films: Ceramic Transactions*; Lu, K., Li, C.; Medvedovski, E., Olevsky, E. A., Eds.; Wiley: New York, 2010; Vol. *223*, pp 1−7.
(44) Wu, J. C.; Shi, W. W.; Chopra, N. *J. Phys. Chem. C.* **2012**, *116*, 12861.
(45) Guo, Y. G.; Wan, L. J.; Bai, C. L. *J. Phys, Chem. B* **2003**, *107*, 5441.
(46) Zhou, X.; Yin, Y. X.; Wan, L. J.; Guo, Y. G. *Adv. Energy Mater.* **2012**, *2*, 1086.
(47) Yang, S. B.; Feng, X. L.; Ivanovici, S.; Mullen, K. *Angew. Chem., Int. Ed.* **2010**, *49*, 8408.
(48) Myung, S.; Solanki, A.; Kim, C.; Park, J.; Kim, K. S.; Lee, K. B. *Adv. Mater.* **2011**, *23*, 2221.
(49) Wang, Y.; Li, Z. H.; Hu, D. H.; Lin, C. T.; Li, J. H.; Lin, Y. H. *J. Am. Chem. Soc.* **2010**, *132*, 9274.
(50) Tang, L. H.; Wang, Y.; Liu, Y.; Li, J. H. *ACS Nano* **2011**, *5*, 3817.
(51) Sun, Y. X.; Zeng, X.; Meng, Q. F.; Zhang, X. Z.; Cheng, S. X.; Zhuo, R. X. *Biomaterials* **2008**, *29*, 4356.
(52) Ren, T. B.; Li, L.; Cai, X. J.; Dong, H. Q.; Liu, S. M.; Li, Y. Y. *Polym. Chem.* **2012**, *3*, 2516.
(53) Chithrani, B. D.; Ghazani, A. A.; Chan, W. C. W. *Nano Lett.* **2006**, *6*, 662.
(54) Bartczak, D.; Muskens, O. L.; Nitti, S.; Elsner, T. S.; Millar, T. M.; Kanaras, A. G. *Small* **2012**, *8*, 122.